

Nanofibers Polyaniline Heterojunction Solar Cell

Tariq J. Alwan¹, Kareema M. Ziadan², Kadhum J. Kadhum³, Muna M. Abbas⁴

¹ALMustansiriyah University, College of Education, Physics Department, Baghdad, Iraq

²University of Basrah, College of Science, Physics Department, Basrah, Iraq

³ALMustansiriyah University, College of Science, Physics Department, Baghdad, Iraq

⁴Baghdad University, College of Science, Physics Department, Baghdad, Iraq

E-mail: tariqjaffer2000@yahoo.com

Received 28 November 2016

Abstract. Organic/inorganic hetero junction solar cells were fabricated by deposition of PAni.CSA/PEO nano fibers on TiO₂ n-type layer by using electrospinning technique. The current-voltage (I-V) measurements of the device under dark conditions exhibit asymmetrical and rectifying behavior for ITO/TiO₂/PAni.CSA.PEO/Al junction that confirms the formation of diode. The diode parameters such as rectification ratio R_r, saturation current I₀, ideality factor n* are determined from I-V curves. The photovoltaic properties of ITO/TiO₂/(PAni.CSA/PEO)/Al junction were studied under illumination condition, and found the short circuit current density J_{sc}= 0.82 mA, open circuit voltage V_{oc} = 485mV, and solar cell efficiency of 0.902 after annealing.

Keywords: Electrospinning, PAni.CSA/PEO, solar cells, nanofibers

1. Introduction

The increasing demands for energy and the limited supply of fossil fuels, the search for alternative sources of power is imperative. Given that, there is a vast amount of energy available from the sun, devices that convert light energy into electrical energy are becoming increasingly important. Solar cells convert light energy into useful electrical power. Polymer photovoltaic is a discovery that potentially houses the solutions to many of the problems currently encountered with traditional photovoltaic technologies. Most notably, the technology offers the possibility for ultrafast processing, low cost, lightweight, flexibility and a very low thermal budget [1]. In these cells their two layers, one containing electron accepting molecules, while the other one containing electron donating layers are used. Majority of the light is absorbed by the electron-donating layer and creates excitons. The excitons have to dissociate to form free charge carriers and this process takes place at the two layers interface and due to the relatively high-energy difference between these layers, the dissociation process is greatly enhanced. Two individual layers separates the electron and hole transportation, greatly reducing the recombination. Moreover, since active region in which splitting process takes place extends into both the accepting and the donating layers, it is almost double compared to single layer cells. Moreover, using two different semiconductors allows the band gaps to be tuned to match better the solar spectrum [2].

Even if the donor and acceptor have an ideal electronic relationship, the performance of bulk hetero junction solar cells still depends on the physical interaction of the donor and acceptor components, which is manifested by the composite morphology. The ideal bulk heterojunction solar cell is defined as a bi-continuous composite of donor and acceptor with a maximum interfacial area for exciton dissociation and a mean domain size commensurate with the exciton diffusion length (5–10 nm). The two components should phase-segregated on a suitable length scale to allow maximum ordering within each phase and thus effective charge transport in continuous pathways to the electrodes so as to minimize the recombination of free charges [3-4].

The aim of this work is the fabrication of ITO/TiO₂/PAni.CSA.PEO/Al heterojunction solar cell, by using the PAni.CSA/PEO nano-fibers as the active organic material, on Al and ITO

electrodes, then to study the various parameters of heterojunction solar cell and the effect of annealing on those parameters.

2. Experimental

Organic/inorganic heterojunction fabricated as below. First, preparation of TiO_2 slurry by mixing 0.6 g of nano TiO_2 (MKnano Comp.) in 3 ml of acetic acid. TiO_2 layer was deposited on the surface of the ITO glass substrate (the sheet resistance is 15 ohm/sq) by manual spread method. The slurry was spread and allowed to dry on the surface. The ITO/ TiO_2 was sintered at 473 K for 30 min. Then deposited the PANi.CSA/PEO nanofiber on TiO_2 layer, with 30% PEO concentration by electrospinning technique. The details of processing have been previously described in ref. [5].

Using glass slide coating by aluminum film via thermal evaporation method. placing the slide facedown (aluminum face) on top of the ITO/ TiO_2 /(PANi.CSA/PEO) side of the other slide, in such a way that the two slides are offset, and using binder clips to attach the two slides, to get ITO/ TiO_2 /(PANi.CSA/PEO)/Al heterojunction solar cell, as presented in Fig. 1.

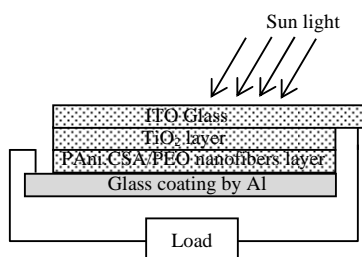


Fig. 1. A schematic of the solar cell layers.

Micropipette was used to fill the space between the two electrodes with the electrolyte iodide/triiodide (I^-/I_3^-) solution. The space between the glass electrodes should turn slightly yellow. To study the effect of annealing, the ITO/ TiO_2 /(PANi.CSA/PEO)/Al heterojunction was annealed at 333 K for 30 min. before adding the electrolyte solution. The surface morphologies of the films were investigated by atomic force microscopy (AFM) (AA3000 Angstrom advanced Inc.). The diode junction current-voltage (I-V) characteristics were measured in the range of (1V)-(-1V) and at steps of 0.1V.

3. Results and Discussion

The morphology, nano-fibers diameters and alignment of PANi.CSA/PEO nano-fibers were examined using AFM. Figure 2 shows the AFM images of PANi.CSA/PEO blend nanofibers with weight ratio concentration of PEO 30 wt.%. The electrospinning of nanofibers from doped PANi.CSA soluble in CHCl_3 did not possible without the addition of PEO to PANi.CSA dissolved in chloroform, no fibers formation occurred, as the viscosity and surface tension of the solution were not high enough to maintain a stable drop at the end of the capillary tip.

The average diameter of PANi.CSA/PEO nanofibers at 30 wt% PEO was about 92.35 nm. It can be also seen from these images that there are fibers, which are free from defects such as beads, relatively smooth with a generally uniform thickness along the fiber. In addition obtained uniaxially aligned nanofibers and the aligned between the more than parallel fibers is constant over large distances as seen in the images. Also the length of nanofiber continues along the test area which closes to 2 μm as shown in Figure 2.

Figure 3 shows the dark I-V characteristic of ITO/ TiO_2 /(PANi.CSA/PEO)/Al heterojunction at room temperature for as spun and annealing samples. It is observed that I-V characteristic of heterojunction is completely unsymmetrical with respect to the polarity of the applied voltage. The curve follows rectifying behavior. This nonlinear increase in current with applied voltage is

explained by the conduction mechanism of polyaniline. Here charge conduction is carried out by the formation of polarons and bipolarons in energy gap [6].

Figure 3 shows a clear rectification which indicates that the junction is aniso-type. The rectification factor indicates the ratio between forward and reverse current at certain applied bias voltage, and Table (1) explains the value of rectification factor at 1 V. The Table also shows an increase in rectification with annealing, and this is attributed to improve in crystal structure with annealing [7].

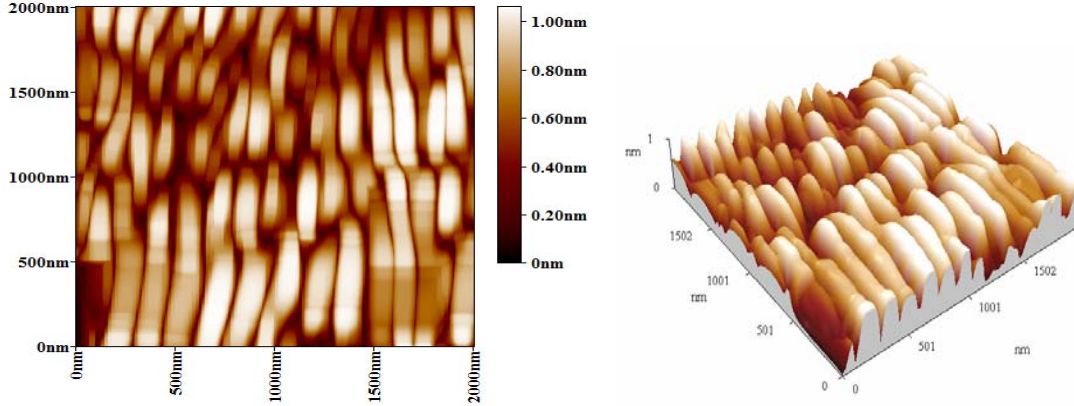


Fig. 2. AFM images of PANi.CSA/PEO electrospun nanofibers.

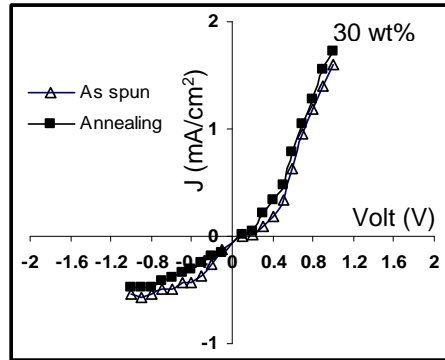


Fig. 3. The dark J-V characteristics of as spun and annealed ITO/TiO₂/(PANi.CSA/PEO)/Al heterojunction.

Thus, the voltage dependence of the junction current can be expressed in the simplified form as [8]:

$$\ln J = \ln J_s + \left(\frac{qV}{n^* k_B T} \right) \quad (1)$$

The J_0 is the saturation current density, and is given as

$$J_s = A^* T^2 \exp\left(-\frac{q\Phi_b}{k_B T}\right) \quad (2)$$

where A^* the effective Richardson constant usually taken as $120 \text{ A}/(\text{cm.K})^{-2}$ for free electrons and Φ_b is the barrier height of the heterojunction.

The saturation current density which can be obtained by extrapolation of the linear $\ln(J)$ - V portion to the $\ln(J)$ axis at zero voltage, the parameters J_s and n^* can be readily determined from the curve shown in Figure 4, together with eq. (1). The values of J_s and n^* are calculated and listed in Table (1) which shows the value of the ideality factor between 2.61-2.75, which is in the same order of $n^* \sim 2.31$ received by B. Boyarbay et al., 2011 [9] for PANi/TiO₂/p-Si heterojunction.

Deviation of n^* far from unity may be attributed to either recombination of electrons with holes in the depletion region, and/or the increase of the diffusion current due to increase in the applied voltage. The higher values of the ideality factor, $n > 2$, in our prepared junctions may be attributed to factors such as interfacial layer thickness, leakage, shunting, bulk series resistance, or any resistive loss [8].

In the second region (higher voltage), other conduction mechanism seems to be predominant. It is observed that the current shows a power dependence on voltage. This power dependence suggests that the dominated dark current is a space-charge-limited current (SCLC) [10].

The Table (1) also includes the values of the barrier height Φ_b , that calculated by eq (2).

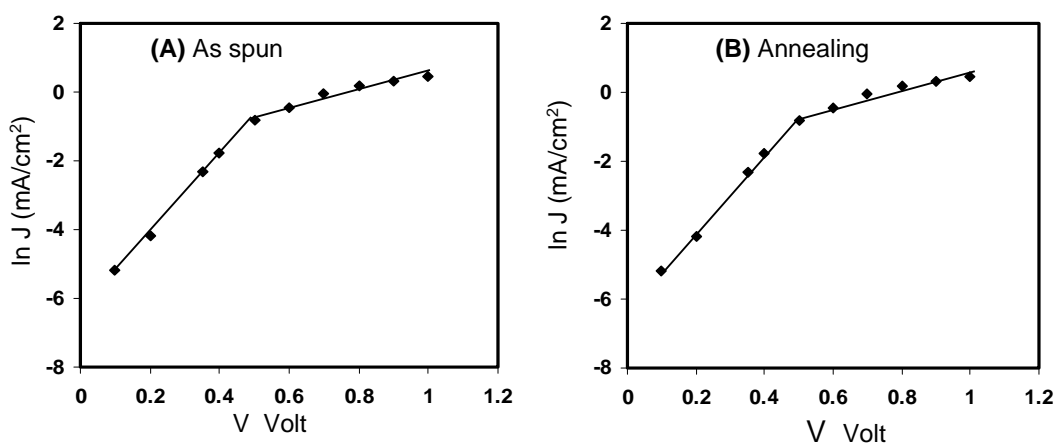


Fig. 4 (A, B). The $\ln J$ - V characteristics at forward bias voltage for ITO/TiO₂/(PANi.CSA/PEO)/Al heterojunction.

Figure 5 shows I - V curves of ITO/TiO₂/(PANi.CSA/PEO)/Al under 100 mW/cm² illumination. From figure (5) and Table (2) it is observed that the photocurrent increases by the annealing from 0.78 mA to 0.82 mA. We assume that the annealing process leads to the decreasing of the energy gap and increases the conductivity, which reduce the main free path of the carrier, which leads to the increase in the photocurrent. Other researchers did the similar description as well [11].

The short circuit current J_{cs} is referred to as the photocurrent J_{ph} , because there is a current at zero external applied voltage. It is as if there was a short circuit in the system [11].

From the obtained result can recognize an increase in V_{oc} with the annealing (see Table 2). This occurs due to the improvement of the crystalline structure and the increase in the conductivity of PANi.CSA/PEO with annealing. This is in agreement with W. Wang et al., 2007 [12] that found the open-circuit voltage V_{oc} increases with the increase of its conductivity for the polyaniline in the solar cells.

The fill factor for ITO/TiO₂/(PANi.CSA/PEO)/Al was calculated by the equation:

$$FF = \frac{P_{\max}}{V_{oc} I_{sc}} = \frac{V_{\max} I_{\max}}{V_{oc} I_{sc}} \quad (3)$$

where P_{max} is the maximum electrical power obtained; I_{sc} and V_{oc} are the short-circuit current density and the open circuit voltage, respectively [13].

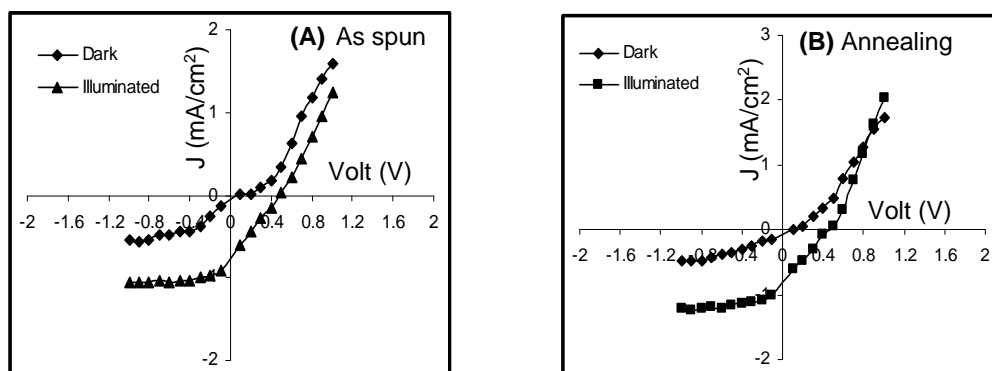


Fig. 5 (A, B). Dark and under illumination (J - V) characteristics of the ITO/TiO₂/(PAni.CSA/PEO)/Al heterojunction.

The efficiency of a solar cell η is determined as the fraction of incident power, which is converted to electricity and is defined as:

$$P_{max} = V_{oc} I_{sc} FF \tag{4}$$

$$\eta = \frac{V_{oc} I_{sc} FF}{P_{in}} \tag{5}$$

The values of FF and the cell efficiency η for the different solar cell are shown in Table (2).

The maximum power generated by a solar cell depends on the fill factor, therefore it is the important parameter to determine the power conversion efficiency of an organic solar cell. There are several factors that can significantly influence to FF, and these factors interact with each other very intricately. Due to this reason, a deep understanding of FF is quite difficult [14]. Those factors are [15] the voltage drop due to the series resistance of the solar cell R_s , as well as due to the leakage current and characterized by the shunt resistance R_{sh} of a solar cell. The recombination in a non-ideal solar cell results in a decrease of the FF.

From Table (2) we observed that the fill factor and conversion efficiency were increased by the annealing, the solar cells after annealing have higher value of the fill factor and conversion efficiency from the as spun ITO/TiO₂/(PAni.CSA/PEO)/Al, because of the annealing enhancement the electrical and optical properties of PAni.CSA/PEO, and also will cause rearrangement of the interface atoms which leads to the improvement of the junction characteristics.

Table (1) The values of n^* , J_s and Φ_b with different conditions.

As spun ITO/TiO ₂ /(PAni.CSA/PEO)/Al				Annealing ITO/TiO ₂ /(PAni.CSA/PEO)/Al			
J_s A/cm ²	n^*	R_r	Φ_b eV	J_s A/cm ²	n^*	Φ_b eV	R_r
2×10^{-6}	2.61	2.94	0.685	2.8×10^{-6}	2.75	0.677	3.6

Table (2) The parameters of solar cell for as spun ITO/TiO₂/(PAni.CSA/PEO)/Al.

	V_{oc} (mV)	J_{sc} (mA/cm ²)	V_{max} (mV)	J_{max} (mA)	P_{max} (mW/cm ²)	R_s Ω	R_{sh} Ω	F.F	η
As apun	484	0.78	223	0.38	84.7	495	7352	0.224	0.84
Annealing	485	0.82	205	0.44	90.2	340	4405	0.227	0.902

4. Conclusions

An organic–inorganic heterojunction diode based on polyaniline and TiO₂ has been fabricated using electrospinning technique. The current-voltage characteristic of this junction performs a rectifying effect, which is interpreted in terms of the barrier formation at the (PAni.CSA/PEO)/TiO₂ interface. The annealed Al/(PAni.CSA/PEO)/TiO₂/TIO solar cell showed better conversion efficiency of 0.902 compared to as spun 0.84.

References

- [1] F. C. Krebs, *Polymer Photovoltaics a Practical Approach*, (Society of Photo-Optical Instrumentation Engineers, (2008).
- [2] W. Hu, F. Bai, X. Gong, X. Zhan, H. Fu, T. Bjornholm, *Organic Optoelectronics*, (Wiley-VCH Verlag GmbH & Co. KGaA, Germany, 2012).
- [3] T. L. Benanti, D. Venkataraman, *Photosynthesis Research*, **87**, (2006), 73.
- [4] B. C. Thompson, J. M. J. Frechet, *Angewandte Chemie International*, **47**, (2008), 58.
- [5] Tariq J. Alwan, Kareema. M. Ziadan, Kadhum K. Kadhum, *International Review of Physics (I.R.PHY)*, **7**(2), (2013), 185.
- [6] D. Patidar, N. Jain, N. S. Saxena, K. Sharma, and T. P. Sharma, *Brazilian Journal of Physics*, **36**(4A), (2006), 1210.
- [7] Tariq J. Alwan, Kareema. M. Ziadan, Kadhum K. Kadhum, *Nano Science and Nano Technology an Indian Journal*, **8**(1), (2013), 22.
- [8] A. M. Farag, E. A. A. El-Shazly, M. Abdel Rafea, A. Ibrahim, *Solar Energy Materials & Solar Cells*, **93**,(2009),1853.
- [9] B. Boyarbay, H. Cetin, A. Uygun, E. Ayyildiz, *Applied Physics A*, **103**,(2011).89.
- [10] M. M. El-Nahass, A. A. Atta, H. E.A. El-Sayed and E. F. M. El-Zaidia, *Current Organic Chemistry*, **14**,(2010),84.
- [11] P. Wurfel, *Physics of Solar Cells: From Principles to New Concepts*, (Wiley-WCH, Weinheim, 2005).
- [12] W. Wang, E. A. Schiff, *Applied Physics Letters*, **91**, (2007), 133504-1.
- [13] M. M. Byranvand, A. N. Kharat, L. Fatholahi, *Journal of Nanostructures (JNS)*, **2**, (2012), 327.
- [14] B. Qi, J. Wang, *Physical Chemistry Chemical Physics*, **15**, (2013), 8972.
- [15] M. A. Green, *Solar Cells*, (Prince-Hall Inc, England, 1982).